Accepted Manuscript

Carbon Dioxide/brine wettability of porous sandstone versus solid quartz: an experimental and theoretical investigation

Firas Alnali, Ahmed Al-Yaseri, Hamid Roshan, Taufiq Rahman, Michael Verall, Maxim Lebedev, Mohammad Sarmadivaleh, Stefan Iglauer, Ahmed Barifcani

Please cite this article as: F. Alnali, A. Al-Yaseri, H. Roshan, T. Rahman, M. Verall, M. Lebedev, M. Sarmadivaleh, S. Iglauer, A. Barifcani, Carbon Dioxide/brine wettability of porous sandstone versus solid quartz: an experimental and theoretical investigation, *Journal of Colloid and Interface Science* (2018), doi: https://doi.org/10.1016/j.jcis.2018.04.029

Carbon Dioxide/brine wettability of porous sandstone versus solid quartz: an experimental and theoretical investigation

Firas Alnali [a,*], Ahmed Al-Yaseri [b], Hamid Roshan [c], Taufiq Rahman [b], Michael Verall [d], Maxim Lebedev [e], Mohammad Sarmadivaleh [b], Stefan Iglauer [b], Ahmed Barifcani [b]

[a]Department of Chemical Engineering, Curtin University, Perth, Australia

[b]Department of Petroleum Engineering, Curtin University, Perth, Australia

[c]School of Petroleum Engineering, University of New South Wales, Kensington, New South Wales, Australia

[d]RSO CSIRO - Mineral Resources, Perth, Australia

[e]Department of Exploration Geophysics, Curtin University, Perth, Australia

*Corresponding author. E-mail address: f.alnili@postgrad.curtin.edu.au

Abstract

Hypothesis: Wettability plays an important role in underground geological storage of carbon dioxide because the fluid flow and distribution mechanism within porous media is controlled by this phenomenon. CO_2 pressure, temperature, brine composition, and mineral type have significant effects on wettability. Despite past research on this subject, the factors that control the wettability variation for CO_2/water/minerals, particularly the effects of pores in the porous substrate on the contact angle at different pressures, temperatures, and salinities, as well as the physical processes involved are not fully understood.

Experiments: We measured the contact angle of deionised water and brine/CO_2/porous sandstone samples at different pressures, temperatures, and salinities. Then, we compared the results with those of pure quartz. Finally, we developed a physical model to explain the observed phenomena.

Findings: The measured contact angle of sandstone was systematically greater than that of pure quartz because of the pores present in sandstone. Moreover, the effect of pressure and temperature on the contact angle of sandstone was similar to that of pure quartz. The results showed that the contact angle increases with increase in temperature and pressure and decreases with increase in salinity.

1. Introduction

Increases in CO_2 emissions represent a formidable problem given the increases in energy demand and high levels of industry-dependent fossil fuel consumption [1]. Various strategies such as the capture and storage of CO_2 in geological formations can be adopted to minimise CO_2 emissions into the atmosphere. The techniques used to store CO_2 underground include CO_2 injection into deep aquifers [2], CO_2 injection into depleted gas and oil reservoirs [3], and storage of CO_2 in coal seam formations underground [4]. While aquifers have the highest volumetric CO_2 storage capacity, CO_2 storage for enhanced oil recovery (EOR) is a more attractive alternative because of its economic viability.

In this context, reducing CO_2 emissions by carbon underground-storage has been specified as a feasible option [5,6]. Combinations involving carbon geo-storage (CGS) and hydrocarbon recovery schemes can be adopted to improve oil and gas recovery [5,7]. In particular, in CGS, CO_2 is collected from large point-source emitters and compressed; then, it is injected deep underground into geological formations [5]. Briefly, the main problem with CGS is related to the density of CO_2, whereby the lower CO_2 density compared to that of the formation brine causes the CO_2 to flow upward, which in turn leads to CO_2 leaks through the caprock. The following four mechanisms can be employed to prevent CO_2 surface leaks: a) structural trapping [8], b) residual trapping [9], c) dissolution trapping [10], and d) mineral trapping [11].

Wettability can be considered an important factor which influences the residual saturation, capillary pressure, and relative permeability, which in turn control the flow in porous rocks [12–15]. In addition, interfacial interactions can have a significant impact on the process of CO_2 storage in hydrocarbon reservoirs and in saline aquifers [14,16,17], where the relation between the interfacial interactions (interfacial tension, capillarity, and wettability) is represented by the Young−Laplace equation [18].

Roughness of the surface can also influence the apparent contact angle at the boundary between the liquid and the surface, and many examples have been given where wetting of the rough surfaces proved to be difficult because of their large apparent contact area [19,20]. Moreover, theoretically, the contact angle increases with increase in the surface roughness for oil-wet surfaces and decreases with increase in the surface roughness for water-wet surfaces [12–23]. However, these effects are still poorly understood, as many other studies have shown both increasing and decreasing trends with increasing surface roughness [24–26].

The contact angles are often measured on pure mineral samples to investigate the fundamental phenomena behind wettability variations with state variables; however, such measurements might not

be representative of an actual reservoir rock with inherent heterogeneities. In fact, very little work has been conducted on wettability measurements of heterogeneous reservoir samples where surface roughness, interfacial tensions, mineral surfaces, and the pore system play key roles. Therefore, we measured the contact angle of CO_2/brine on a porous sandstone surface under reservoir conditions and analysed the dependency of the contact angle on the pore fraction where the pressure, temperature, and brine salinity were varied. We also developed a physical model to describe the observed phenomena.

2.   Experimental methodology

A sandstone sample from well 2 in the Warro gas field was used for this study. The Warro field is situated in a convenient location onshore in the Perth Basin, approximately 200 km north of Perth, Australia, where the in-place reserve is estimated to be 7–10 trillion cubic feet (TCF) and a large amount (1–3 TCF) of potentially recoverable gas is present. The field structure is a large, simple, closed, growth-type anticline with no major faulting activities. The Warro-2 well was drilled to check the productivity potential of the Yarragadee Formation, and the well's depth reached 4854 m by early 1978. The well has undergone a considerable number of tests including fracturing, wireline logging, conventional and side wall coring, formation pressure, and temperature analyses. Several conventional cores were cut. In this research, we used a core sample from the depth of 3836.2 m with a porosity and air permeability of 9.6% and 0.5 md, respectively. The composition of the sandstone sample was measured via x-ray diffraction (XRD) with a Bruker-AXS D9 Advance Diffractometer (quartz 90 wt%, kaolin 3.3 wt%, feldspar 6.7 wt%), and the results indicated that the sandstone sample was composed mainly of quartz. Furthermore, the total organic content (TOC) was 0.16 wt%, which is indicative of poor organic richness [27]. The root mean square (RMS) of surface roughness (540 nm) was measured with an atomic force microscope, instrument model AFM DSE 95-200 (Fig. 1). In addition, scanning electron microscopy-energy dispersive x-ray spectroscopy (SEM-EDX) was used to estimate the surface solid fraction (f = 0.65) by using Avizo software (the raw images were filtered with a non-local mean filter, and then, images were segmented by using watershed segmentation methods) (Fig. 2). Air plasma was used for 5 min to clean the sample and remove surface contamination [28] following the procedures of Iglauer et al. [29] and Sarmadivaleh et al. [30]. This cleaning procedure is essential to obtain accurate results and avoid any errors [29,31]. The cleaned sample was then placed in a pressure cell (Fig. 3) at the required temperature (296, 323, and 343 K). By using a high precision syringe pump (ISCO 500D; pressure accuracy of 0.1% FS), CO_2 was then injected into the chamber and the pressure was raised to pre-set values (0.1, 5, 10, 15, and 20 MPa). Notably, CO_2 was used to saturate the brine by using a mixing reactor [32]. However,

according to a previous study [33], such an equilibration (CO_2–brine solubility equilibration) has no significant effect on the contact angle measurement.

When the pressure reached the set pressure, a single deionised (DI) water or brine (20 wt% $CaCl_2$) droplet (average volume of a single drop was ~6 ± 1 μL) was passed onto the sandstone via a needle. Moreover, the tilting-plate technique was applied to measure the contact angle [34–36], as this technique can simultaneously measure advancing and receding events under the same circumstances. An earlier study [35] proved that the tilting plate method offers more reliable data than the sessile drop technique. In this study, a tendency angle of $\alpha = 12°$ for the sample, which was placed on a metal platform into the pressure chamber, was attained. Under such a condition, the slightest movement of the droplet from the upper side to the lower side of the substrate will occur as result of the gravitational force.

The measurement of the advancing water contact angle (θ_a) was achieved at the front of the droplet prior to droplet movement, and the measurement of the receding (θ_r) water contact angle was attained at the trailing edge of the droplet. In this case, the gravity is pointless, as the radius of the water droplet contact length was ≈ 1.7 ± 0.2 mm under the capillary length. The entire process was recorded with a high-resolution camera (Basler scA 640–70 fm, pixel size = 7.4 μm; frame rate = 71 fps; Fujinon CCTV lens: HF35HA-1B; 1:1.6/35 mm), and the extracted images taken from the video were used to measure θ_a and θ_r [37].
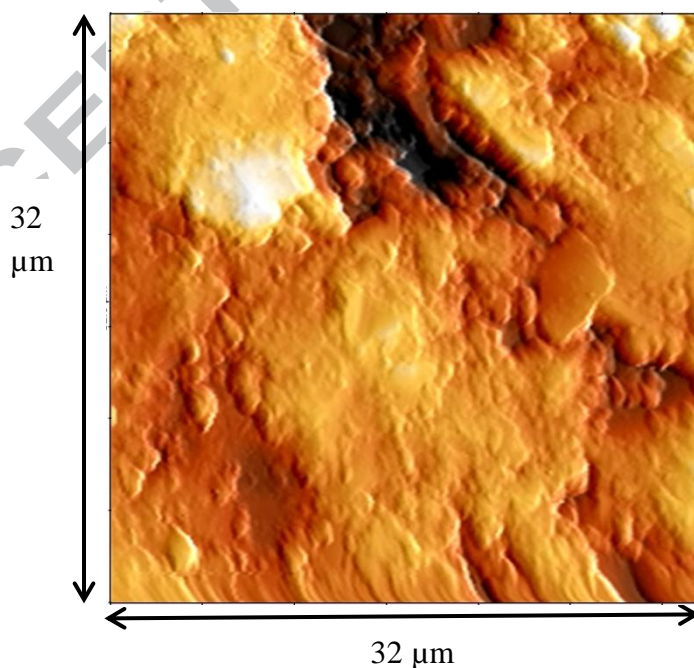
Figure 1. Atomic force microscopy image of the sandstone surfaces investigated; different heights are coloured differently (black is 0 nm, white is 3500 nm).
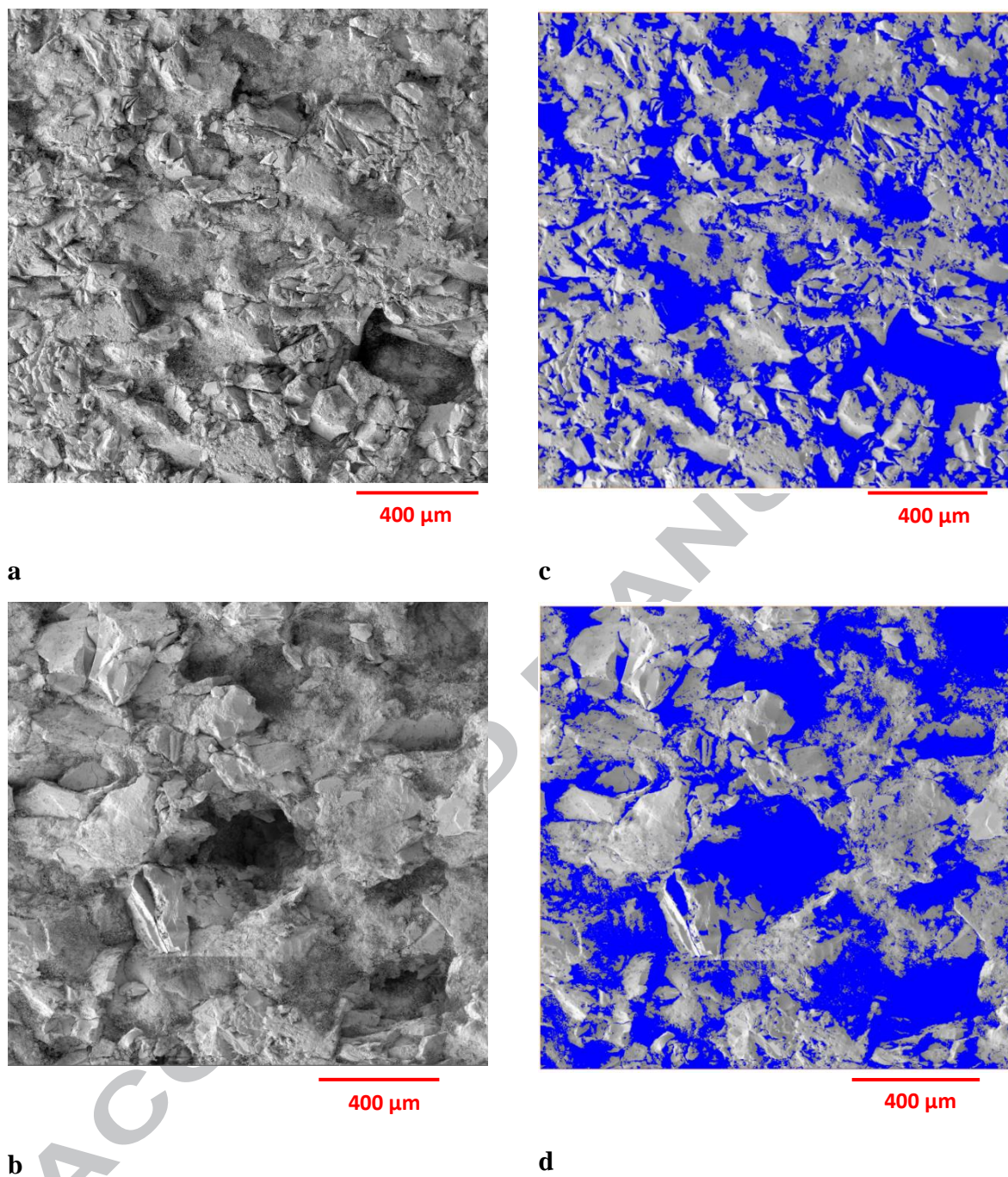
Figure 2. SEM images of the sandstone samples; a and b are the raw images and c and d are the segmented images. Grey shows the grains, while blue shows the pores.

Contact angle measurement chamber
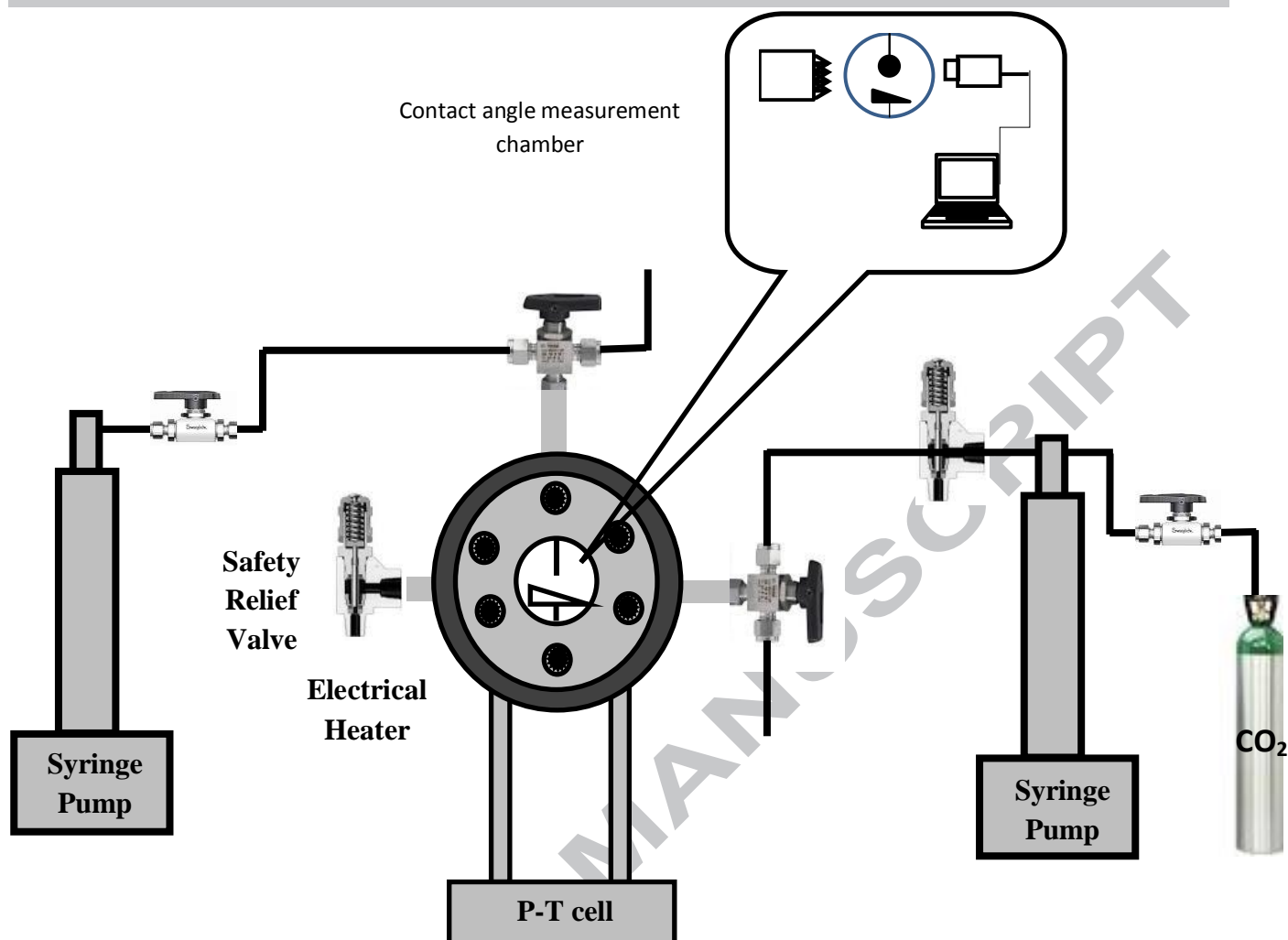
Figure 3. Schematic diagram of the high temperature/high pressure contact angle measurement apparatus used for contact angle measurements.

3. Results

Water contact angle (θ) was measured at various set pressures (0.1, 5, 10, 15, and 20 MPa) and temperatures (296, 323, and 343 K) on a sandstone surface (RMS surface roughness = 540 nm). The advancing and receding contact angles under ambient conditions (T = 296 K and 0.1 MPa CO_2 pressure) were close to zero, similar to previous reports [29,38]. However, advancing and receding contact angles increased with the increasing pressure (Figs. 4a and 4b), which is consistent with measurements reported in the literature [21,29,30,33]. The advancing–receding contact angles of quartz [21] were plotted along with those of sandstone for comparison purposes. Iglauer et al. [39] explained this behaviour by invoking the rapid increase in CO_2 density with pressure, which strengthens the intermolecular interactions between CO_2 and quartz and thus leads to de-wetting of the surface [18,37]. Further, advancing and receding contact angles were observed to increase with the increasing temperature (Figs. 4a and 4b) [18,21,30,40].

The effect of salinity on the contact angle was also investigated at 323 K and various pressures (5, 10, 15, and 20 MPa). Deionised water and 20 wt% $CaCl_2$ were used to observe the effect of ion concentration on the sandstone contact angle. The advancing and receding contact angles were increased by ~10° and ~12°, respectively, when 20% $CaCl_2$ was used in comparison to DI water at 5 MPa (Figs. 5a and 5b). The advancing and receding contact angles were also increased when $CaCl_2$ was used for all other pressures, namely, 10, 15, and 20 MPa (Figs. 5a and 5b). Thus, more concentrated brine resulted in higher contact angles when compared to DI water, which is consistent with previous studies [21, 31, 40, and 41]. Chemicals purity are presented in table 1

| Chemical Name	Source of Supply	State	Purity (wt. %)
CO_2	BOC Australia	Gas	≥ 0.999
$CaCl_2$	Scharlab, Spain	Powder	≥ 0.995
DI Water	David Gray's Deionized	Liquid	[a] Conductivity (0.02 mS/cm)

[a] The conductivity of DI water was measured with Multiparameter (HI 9823) at T= 294 K.
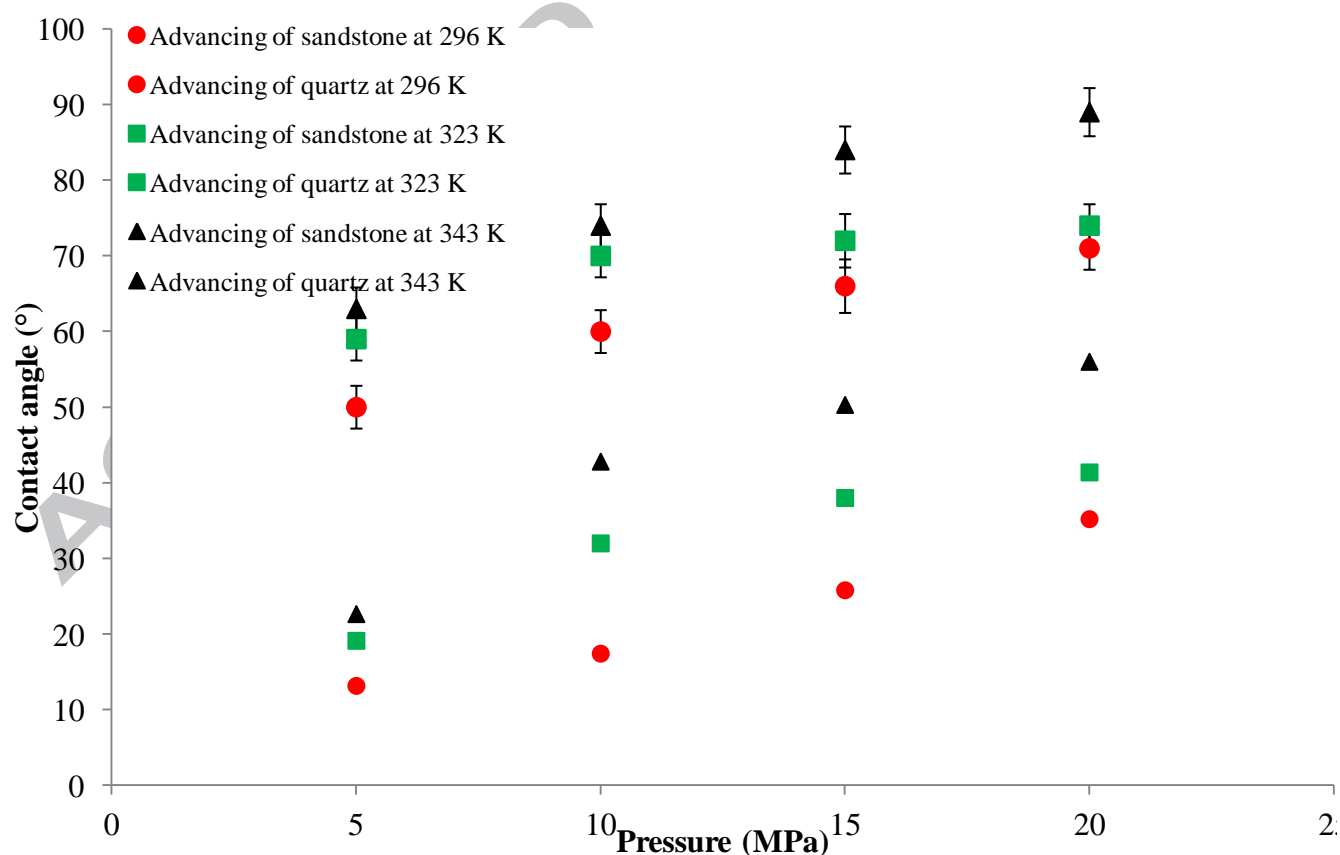
Figure 4a. Advancing water contact angles for sandstone/CO_2/DI water as a function of pressure and

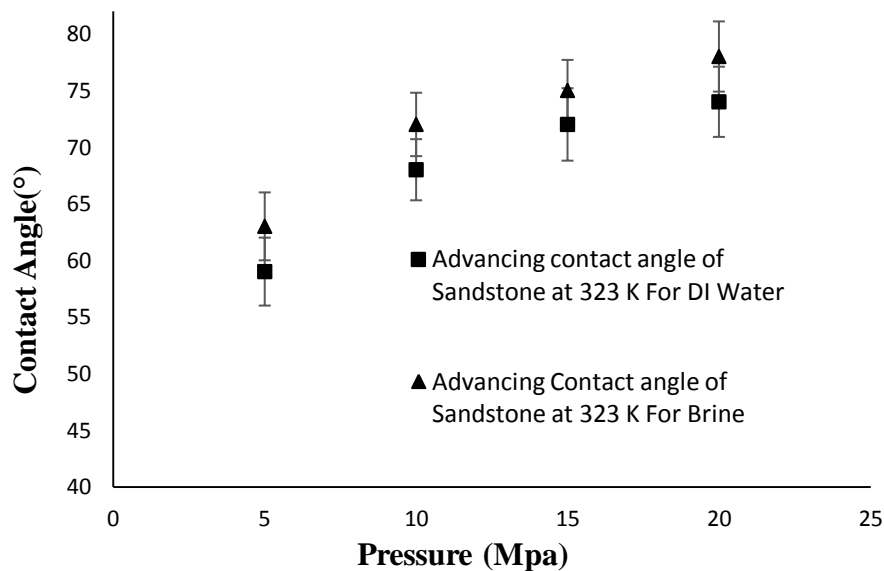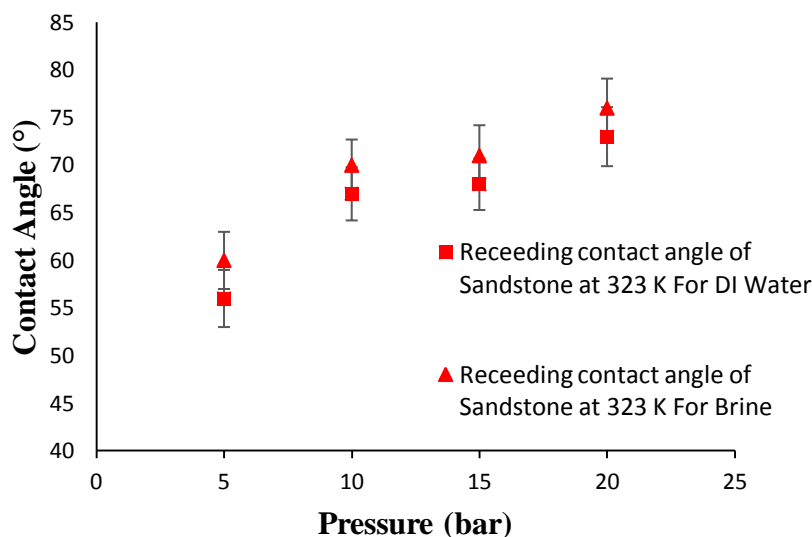temperature; RMS = 540 nm, SD = 3 (where SD is the standard deviation).
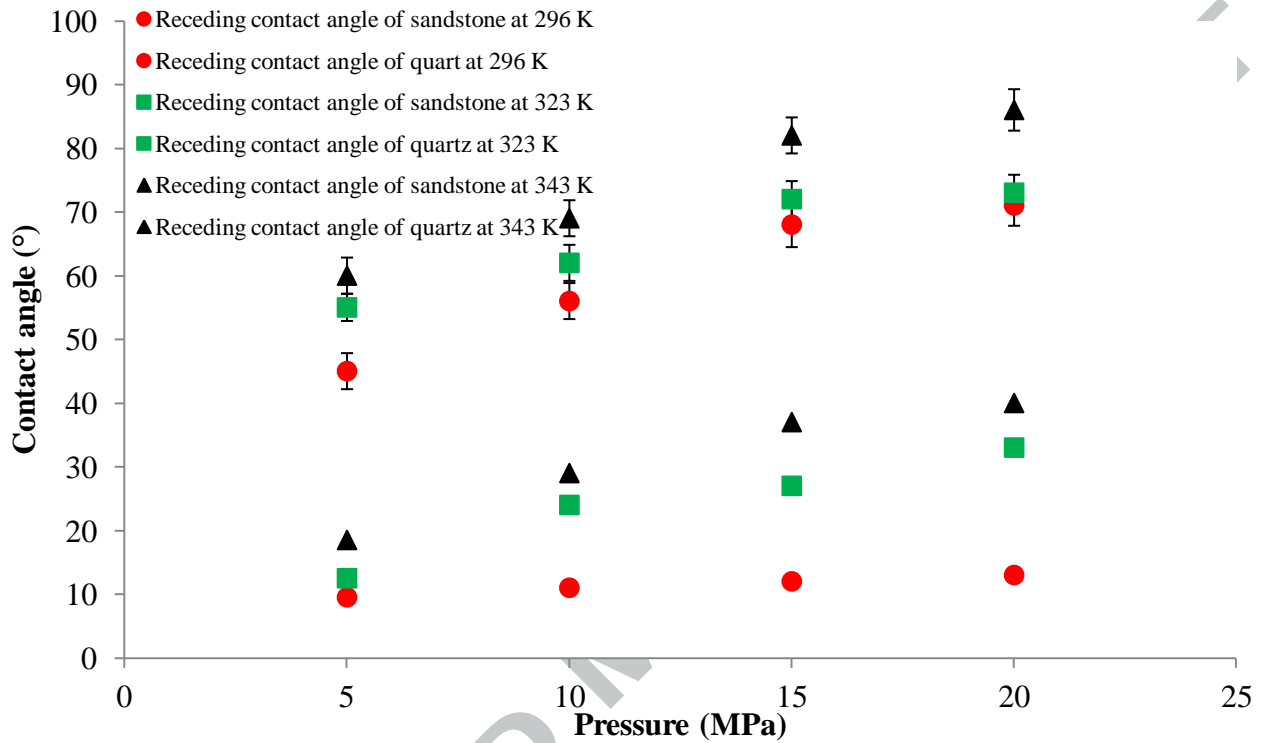
Figure 4b. Receding contact angles for sandstone/CO_2/DI water as a function of pressure and temperature; RMS = 540 nm, SD = 3.

Figure 5a. Advancing contact angles for sandstone/CO_2/DI water and sandstone/CO_2/brine (20 wt% $CaCl_2$) as a function of pressure at a temperature of 323 K; RMS = 540 nm, SD = 3.

Figure 5b. Receding contact angles for sandstone/CO_2/DI water and sandstone/CO_2/brine water (20 wt% $CaCl_2$) as a function of pressure at a temperature of 323 K; RMS = 540 nm, SD = 3.

4.   Discussion

We first recall the contact angle measurements of pure quartz at different pressures and temperatures published by Al-Yaseri et al. [21]. These extracted data are consistent with other contact angles reported for quartz [42,43]. These data are presented in Fig. 6 along with our contact angle measurements of porous sandstone. It can be seen from Fig. 6 that the water contact angle of sandstone is consistently higher than that of pure quartz (which has no pores) regardless of the pressure and temperature of the system, and these data are consistent with the porous sandstone contact angle data presented by Cassie et al. [19]. While pressure increases the contact angle for both sandstone and quartz, this effect is more pronounced at lower temperatures. Temperature has a minimal effect on the contact angle. It increases only slightly with increasing temperature.

To analyse such differences between the contact angles of sandstone and quartz caused by the presence of pores, we assume that sandstone is mainly composed of quartz, i.e. the pores are also filled with CO_2 at the beginning of the experiment. Further, the TOC was very low (0.16 wt%) [27] for the selected sandstone sample, which makes it more suitable for CO_2 storage [44]. Notably, Arif et al. [45] observed a clear relationship between the TOC and CO_2-wettability of the rock, whereby a high TOC content can lead to a high water–CO_2 contact angle (lower water wettability).

When a drop of liquid, in the presence of another fluid (liquid or gas), is dispended on a solid surface with no/minimal electric potential, the droplet spreads across the solid surface until the minimum free energy is reached [46]. This is related to the cohesion forces in the fluids and adhesion forces between the fluid material and the solid surface. If the energy dissipation due to the movement

of the contact line by hysteresis is neglected, and the free energy change due to an infinitesimal increase in the base area of the droplet on the solid surface (surrounded by another fluid) is considered, the free energy of the system can be calculated as follows [46]:

$$dF = \gamma_{LG} \cos\theta dA - \gamma_{SG} dA + \gamma_{SL} dA \tag{1}$$

where γ is the interfacial tension or surface free energy, F is the total free energy of the system, θ is the contact angle of the droplet, and dA is the infinitesimal surface area (s, g, and L represent the solid, gas and liquid phases, respectively). When the minimum energy is attained and equilibrium is established, Eq. (1) turns to a special case, Young's equation [18].

When the solid quartz surface is considered (Fig. 6), Young's equation is assumed to explain the force equilibrium in the droplet [37]:

$$\gamma_{LG} \cos\theta = \gamma_{SG} - \gamma_{SL} \tag{2}$$

However, when pores exist within the substrate, extra capillary forces, driven by water movement into pores, exist (if the substrate is water-wet). We call this force f herein (Fig. 6). This force is a result of the capillary pressure (Δp) acting on pores underneath the droplet ($\phi.dA$). The infinitesimal capillary force acting on pore space can then be written as follows:

$$f = \Delta p(\phi.dA) \tag{3}$$

where Δp is the capillary pressure. The energy associated with the infinitesimal capillary rise (f_C) then takes the following form:

$$f_C = \Delta p(\phi.dA).\tilde{h} \tag{4}$$

where $\tilde{h}$ is the average capillary rise in the pore system. Substituting capillary pressure with $\frac{2\gamma_{LG} \cos\theta}{\tilde{r}}$ (where $\tilde{r}$ is the average pore radius) yields:

$$f_C = \frac{2\gamma_{LG} \cos\theta}{\tilde{r}} \tilde{h}(\phi.dA) \tag{5}$$

Therefore, the free energy equation takes the form:

$$dF = \gamma_{LG} \cos\theta dA - \gamma_{SG} dA + \gamma_{SL} dA + f_C \tag{6}$$

Thus, the energy equilibrium equation ($dF \to 0$) yields:

$$\gamma_{LG} \cos\theta = \gamma_{SG} - \gamma_{SL} - \frac{2\phi\gamma_{LG} \cos\theta}{\tilde{r}} \tilde{h} \tag{7}$$

Eq. 7 illustrates that the contact angle of porous sandstone must be higher than that of pure quartz if other thermodynamic variables such as pressure and temperature are unchanged. This is supported by the experimental data of the porous sandstone investigated in this study when compared to that of

solid quartz reported by Al-Yaseri et al. [21]. In addition, the experimental contact angles for porous sandstone reported by Kaveh et al. [47] were higher than the contact angle for pure quartz consistent with those reported by Al-Yaseri et al. [21], Espinoza et al. [42], and Chiquet et al. [43]. In all cases, the contact angle of sandstone is consistently higher than that of quartz.

In order to justify our approach, we have taken images from a water droplet on the sandstone sample after 2 and 4 min (Fig. 7). It is evident from this figure that water started to migrate into the pores, which clearly demonstrates that a capillary force is active.

With increases in the elapsed time, more water infiltrated, and the contact angle decreased significantly from 55° to 45°, which indicates that the capillary-driven force (f) weakened with time until it reached equilibrium (Fig. 7). It should be noted that at equilibrium, the contact angle of porous sandstone was still higher than that of pure quartz. However, if pore walls are hydrophobic, the contact angle will stay unchanged with no/minimal water entry into the pores [48].

It is thus clear that porous water-wet substrates exhibit higher water contact angles (when compared with identical surfaces without pores).

We furthermore conclude that the amount of surface pores (porosity fraction), pore throat diameter, and height of fluid infiltration play important roles in the magnitude and kinetics of contact angle variation on porous surfaces. This is caused by the driving capillary forces, which can affect CO_2 residual trapping during spontaneous imbibition for both carbon sequestration and enhanced oil recovery [49,50].

We now consider the Cassie–Baxter equation (Eq. 8) to assess its accuracy in predicting measured sandstone contact angle data. We also consider the effect of pressure and temperature on the fluid interfacial tension to assess its contact angle prediction capability (Fig. 8). The Cassie–Baxter equation was used to predict the trend of contact angle changes. However, as can be seen from Fig. 8, the obtained contact angles were significantly out of range. We then used the same set of variables (porosity = 9.6%) assuming that h is known (0.5 mm from Fig. 7) to predict the sandstone contact angles (also plotted in Fig. 8) with our newly derived equation (Eq. 7). It can be seen from Fig. 8 that the predicted contact angle of our equation was close to the measured value and displayed the same trend as that of the Cassie–Baxter equation:

$$\cos\theta_c = f_i \cos\theta - (1 - f_i) \tag{8}$$

where θc is the predicted Cassie–Baxter contact angle, f_i is the fractional projected area of material, θ is the smooth area contact angle, and ($1-f_i$) is thought to reflect the contribution of air remaining under the droplet [51].

The only parameter which externally influences the contact angle in the Cassie–Baxter equation is porosity, which means that the analysed prediction is the best outcome of this model for the current data set. Our equation however takes into account the pore radius and water infiltration height along with the porosity. Porosity and average pore radius data are often available for tested samples, but not the infiltration height. While having this parameter will significantly improve model predictions of a porous substrate, the wettability information is required to estimate this parameter precisely. The other approach is to use correlation based estimations of h which can be obtained with data sets of a particular substrate. For instance, the correlation of h can be calculated with respect to other state variables and the results can be applied to new data sets. Determining such a correlation or an alternative physical equation as a function of state variables will therefore be a future research direction.
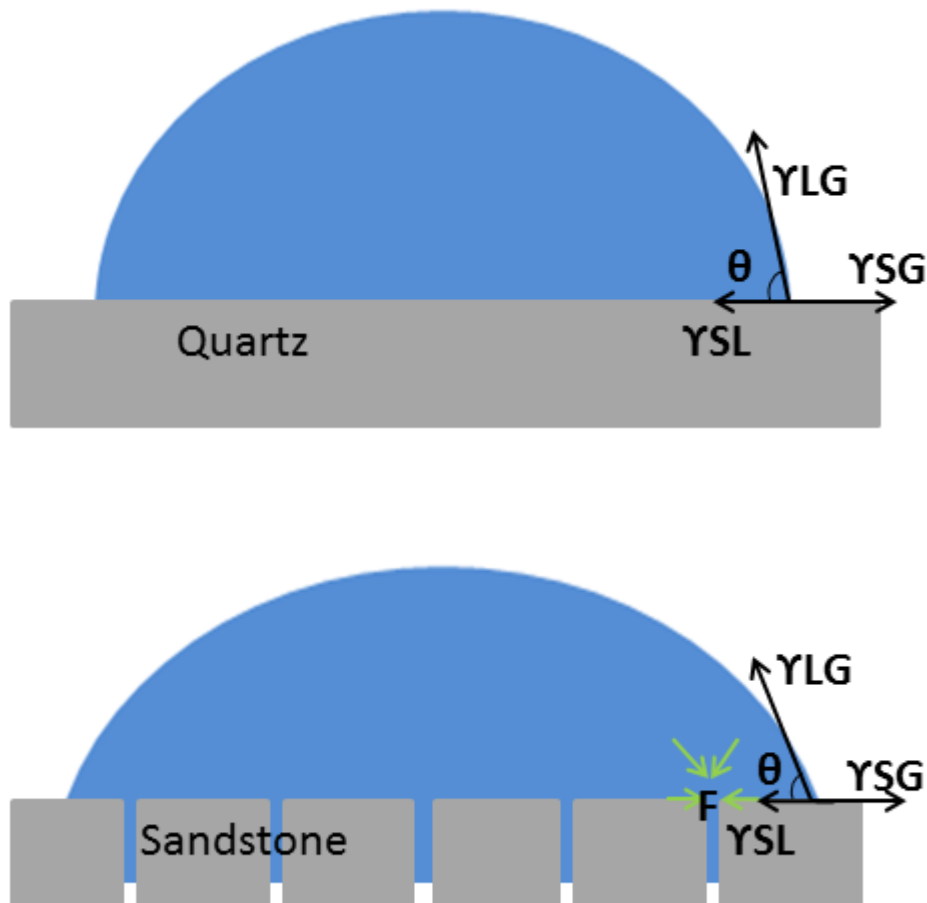
Figure 6. Forces acting on quartz (top) and sandstone (bottom).
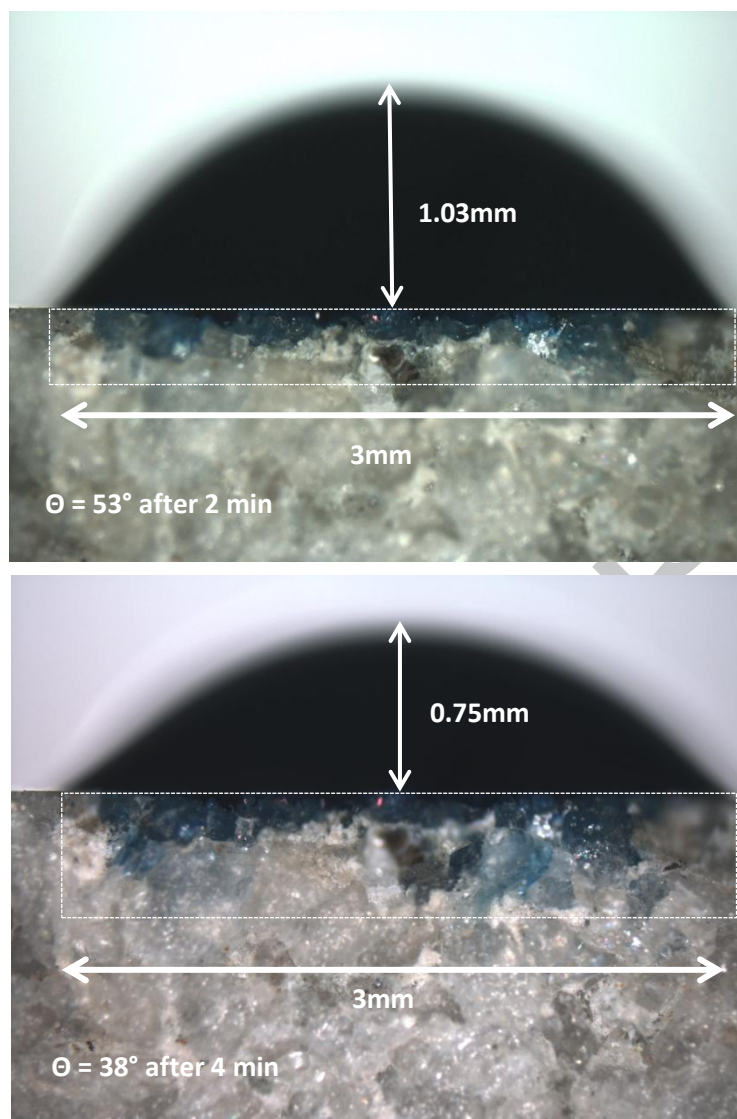
Figure 7. Water droplet on a sandstone sample in the presence of air under atmospheric conditions after exposure times of 2 min (top) and 4 min (bottom).
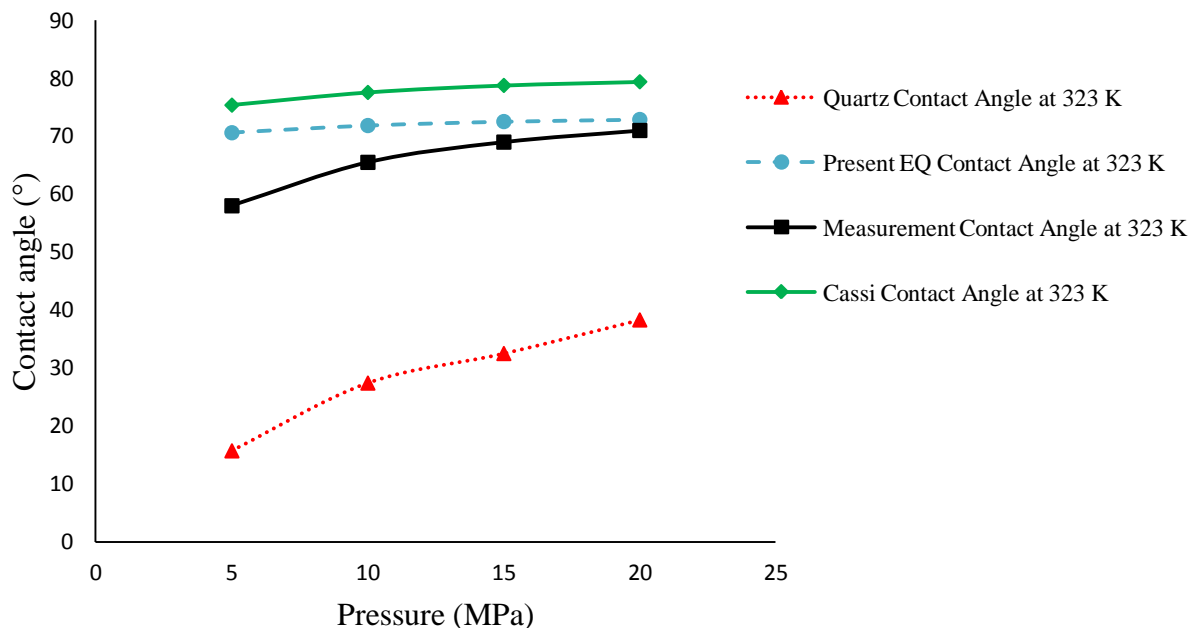
Figure 8. Comparison of the equilibrium contact angles obtained through laboratory experiments, the Cassie–Baxter method, and the present method at a temperature of 323 K.

5. Conclusions

Pore systems and surface roughness are considered to be fundamental factors which influence the variations in the wettability of reservoir rock with inherent heterogeneities. The advancing-receding contact angles of brine/CO_2 and sandstone as a function of pressure, temperature, and salinity were investigated in this study. The results were then compared with the contact angles of pure quartz samples measured at the same pressure, temperature, and salinity. It was found that the contact angle of sandstone was systematically higher than that of pure quartz at any pressure or temperature because of the presence of pores in sandstone. The contact angles also increased with increase in pressure and temperature and decreased with increase in the salinity. In addition, the contact angles of porous sandstone determined using the Cassie–Baxter equation were consistent with those determined using our new derived model (Eq. 7). Increase in the contact angle due to the presence of pores was linked to the capillary-driven forces acting at the surface pore throats and were mathematically formulated. The imaging of water entry into the substrate pores with optical microscopy confirmed the validity of the analytical approach adopted. Further studies should be conducted on pore rocks with different pore sizes and structures to better understand the variations in wettability in the presence of porosity.

References

1. IEA (International Energy Agency), *World Energy Outlook Special Report*, 2013, 126 pp.

2. A.E. Ofori, T.W. Engler, Effects of CO_2 sequestration on the petrophysical properties of an aquifer rock. In: *Canadian Unconventional Resources Conference*, Society of Petroleum Engineers, 2011.

3. R.J. Arts, V.P. Vandeweijer, C. Hofstee, M.P.D. Pluymaekers, D. Loeve, A. Kopp, W.J. Plug, The feasibility of CO_2 storage in the depleted P18-4 gas field offshore the Netherlands (the ROAD project), *International Journal of Greenhouse Gas Control* 11 (2012) S10‑S20.

4. F. Van Bergen, P. Krzystolik, N. van Wageningen, H. Pagnier, B. Jura, J. Skiba, P. Winthaegen, Z. Kobiela, Production of gas from coal seams in the Upper Silesian Coal Basin in Poland in the post-injection period of an ECBM pilot site, *International Journal of Coal Geology* 77(1) (2009) 175‑187.

5. IPCC (Intergovernmental Panel on Climate Change), *Working Group III of the Intergovernmental Panel on Climate Change*, 2005, 443 pp.

6. P. Tomski, V. Kuuskraa, M. Moore, *Atlantic Council*, 2013, 15 pp.

7. S. Iglauer, A. Paluszny, M.J. Blunt, Simultaneous oil recovery and residual gas storage: A pore-level analysis using in situ X-ray micro-tomography, *Fuel* 103 (2013) 905‑914.

8. M.A. Hesse, F.M. Orr, H.A. Tchelepi, Gravity currents with residual trapping, *Journal of Fluid Mechanics* 611 (2008) 35‑60.

9. S. Iglauer, A. Paluszny, C.H. Pentland, M.J. Blunt, Residual CO_2 imaged with X-ray micro-tomography, *Geophysical Research Letters* 38(21) (2011) L21403.

10. S. Iglauer,. Dissolution trapping of carbon dioxide in reservoir formation brine–a carbon storage mechanism. In *Mass Transfer-Advanced Aspects*. InTech, 2011.

11. I. Gaus, Role and impact of CO_2–rock interactions during CO_2 storage in sedimentary rocks, *International Journal of Greenhouse Gas Control* 4(1) (2010) 73‑89.

12. W.G. Anderson, Wettability literature survey-Part 1: rock/oil/brine interactions and the effects of core handling on wettability, *Journal of Petroleum Technology* 38(10) (1986) SPE-13932-PA.

13. N.R. Morrow, Wettability and its effect on oil recovery, *Journal of Petroleum Technology* 42(12) (1990) SPE-21621-PA.

14. B. Arendt, D. Dittmar, R. Eggers, Interaction of interfacial convection and mass transfer effects in the system CO_2–water, *International Journal of Heat and Mass Transfer* 47(17) (2004) 3649‑3657.

15. S. Iglauer, CO_2–water–rock wettability: Variability, influencing factors, and implications for CO_2 geostorage, *Accounts of Chemical Research* 50(5) (2017) 1134‑1142.

16. C. Chalbaud, M. Robin, J.M. Lombard, F. Martin, P. Egermann, H. Bertin, Interfacial tension measurements and wettability evaluation for geological CO_2 storage, *Advances in Water Resources* 32(1) (2009) 98‑109.

17. D. Yang, Y. Gu, P. Tontiwachwuthikul, Wettability determination of the crude oil−reservoir brine−reservoir rock system with dissolution of CO_2 at high pressures and elevated temperatures, *Energy and Fuels* 22(4) (2008) 2362‑2371.

18. H. Roshan, A.Z. Al-Yaseri, M. Sarmadivaleh, S. Iglauer, On wettability of shale rocks, *Journal of Colloid and Interface Science* 475 (2016) 104‑111.

19. A.B.D. Cassie, S. Baxter, Wettability of porous surfaces, *Transactions of the Faraday Society* 40 (1944) 546‑551.

20. R.N. Wenzel, Resistance of solid surfaces to wetting by water, *Industrial and Engineering Chemistry* 28(8) (1936) 988‑994.

21. A.Z. Al-Yaseri, M. Lebedev, A. Barifcani, S. Iglauer, Receding and advancing (CO_2 + brine + quartz) contact angles as a function of pressure, temperature, surface roughness, salt type and salinity, *The Journal of Chemical Thermodynamics* 93 (2016) 416‑423.

22. A.B.D. Cassie, Contact angles, *Discussions of the Faraday Society* 3 (1948) 11‑16.

23. Y. Tamai, K. Aratani, Experimental study of the relation between contact angle and surface roughness, *The Journal of Physical Chemistry* 76(22) (1972) 3267‑3271.

24. F.E. Bartell, J.W. Shepard, Surface roughness as related to hysteresis of contact angles. II. The systems paraffin–3 molar calcium chloride solution–air and paraffin–glycerol–air, *The Journal of Physical Chemistry* 57(4) (1953) 455‑458.

25. K.T. Hong, H. Imadojemu, R.L. Webb, Effects of oxidation and surface roughness on contact angle, *Experimental Thermal and Fluid Science* 8(4) (1994) 279‑285.

26. J. Drelich, J.D. Miller, The effect of solid surface heterogeneity and roughness on the contact angle/drop (bubble) size relationship, *Journal of Colloid and Interface Science* 164(1) (1994) 252‑259.

27. G.E. Claypool, P.R. Reed, Thermal-analysis technique for source-rock evaluation: Quantitative estimate of organic richness and effects of lithologic variation: GEOLOGIC NOTES. *AAPG Bulletin* 60(4) (1976) 608‑612.

28. J.C. Love, L.A. Estroff, J.K. Kriebel, R.G. Nuzzo, G.M. Whitesides, Self-assembled monolayers of thiolates on metals as a form of nanotechnology, *Chemical Reviews* 105(4) (2005) 1103‑1170.

29. S. Iglauer, A. Salamah, M. Sarmadivaleh, K. Liu, C. Phan, Contamination of silica surfaces: impact on water–CO_2–quartz and glass contact angle measurements, *International Journal of Greenhouse Gas Control* 22 (2014) 325‑328.

30. M. Sarmadivaleh, A.Z. Al-Yaseri, S. Iglauer, Influence of temperature and pressure on quartz–water–CO_2 contact angle and CO_2–water interfacial tension, *Journal of Colloid and Interface Science* 441 (2015) 59‑64.

31. P.K. Bikkina, Reply to the comments on "Contact angle measurements of CO_2–water–quartz/calcite systems in the perspective of carbon sequestration," *International Journal of Greenhouse Gas Control* 7 (2012) 263‑264.

32. R.M. El-Maghraby, C.H. Pentland, S. Iglauer, M.J. Blunt, A fast method to equilibrate carbon dioxide with brine at high pressure and elevated temperature including solubility measurements, *The Journal of Supercritical Fluids* 62 (2012) 55‑59.

33. A. Al-Yaseri, M. Sarmadivaleh, A. Saeedi, M. Lebedev, A. Barifcani, S. Iglauer, N_2+CO_2+NaCl brine interfacial tensions and contact angles on quartz at CO_2 storage site conditions in the Gippsland basin, Victoria/Australia, *Journal of Petroleum Science and Engineering* 129 (2015) 58‑62.

34. G. Macdougall, C. Ockrent, Surface energy relations in liquid/solid systems I. The adhesion of liquids to solids and a new method of determining the surface tension of liquids, *Proceedings of the Royal Society of London A* 180 (1942) 151‑173.

35. L.M. Lander, L.M. Siewierski, W.J. Brittain, E.A. Vogler, A systematic comparison of contact angle methods, *Langmuir* 9(8) (1993) 2237‑2239.

36. C.W. Extrand, Y. Kumagai, Liquid drops on an inclined plane: the relation between contact angles, drop shape, and retentive force, *Journal of Colloid and Interface Science* 170(2) (1995) 515‑521.

37. A.Z. Al-Yaseri, H. Roshan, M. Lebedev, A. Barifcani, S. Iglauer, Dependence of quartz wettability on fluid density, *Geophysical Research Letters* 43(8) (2016) 3771‑3776.

38. J.W. Grate, K.J. Dehoff, M.G. Warner, J.W. Pittman, T.W. Wietsma, C. Zhang, M. Oostrom, Correlation of oil–water and air–water contact angles of diverse silanized surfaces and relationship to fluid interfacial tensions, *Langmuir* 28(18) (2012) 7182‑7188.

39. S. Iglauer, M.S. Mathew, F. Bresme, Molecular dynamics computations of brine–CO_2 interfacial tensions and brine–CO_2–quartz contact angles and their effects on structural and residual trapping mechanisms in carbon geo-sequestration, *Journal of Colloid and Interface Science* 386(1) (2012) 405‑414.

40. S. Saraji, L. Goual, M. Piri, H. Plancher, Wettability of supercritical carbon dioxide/water/quartz systems: simultaneous measurement of contact angle and interfacial tension at reservoir conditions, *Langmuir* 29(23) (2013) 6856‑6866.

41. R. Farokhpoor, B.J. Bjørkvik, E. Lindeberg, O. Torsæter, Wettability behaviour of CO_2 at storage conditions, *International Journal of Greenhouse Gas Control* 12 (2013) 18‑25.

42. D.N. Espinoza, J.C. Santamarina, Water-CO_2-mineral systems: Interfacial tension, contact angle, and diffusion—Implications to CO_2 geological storage, *Water Resources Research* 46(7) (2010) W07537.

43. P. Chiquet, D. Broseta, S. Thibeau, Wettability alteration of caprock minerals by carbon dioxide, *Geofluids* 7(2) (2007) 112‑122.

44. S. Iglauer, A.Z. Al-Yaseri, R. Rezaee, M. Lebedev, CO_2 wettability of caprocks: Implications for structural storage capacity and containment security, *Geophysical Research Letters* 42(21) (2015) 9279‑9284.

45. M. Arif, M. Lebedev, A. Barifcani, S. Iglauer, Influence of shale-total organic content on CO_2 geo-storage potential, *Geophysical Research Letters* 44 (2017) 8769‑8775.

46. H.J.J. Verheijen, M.W.J. Prins, Reversible electrowetting and trapping of charge: model and experiments, *Langmuir* 15(20) (1999) 6616‑6620.

47. N.S. Kaveh, E.S.J. Rudolph, P. Van Hemert, W.R. Rossen, K.H. Wolf, Wettability evaluation of a CO_2/water/bentheimer sandstone system: contact angle, dissolution, and bubble size, *Energy and Fuels* 28(6) (2014) 4002‑4020.

48. A.Z. Al-Yaseri, H. Roshan, Y. Zhang, T. Rahman, M. Lebedev, A. Barifcani, S. Iglauer, Effect of the temperature on CO_2/brine/dolomite wettability: Hydrophilic versus hydrophobic surfaces, *Energy and Fuels* 31(6) (2017) 6329‑6333.

49. S. Strand, D.C. Standnes, T. Austad, Spontaneous imbibition of aqueous surfactant solutions into neutral to oil-wet carbonate cores: Effects of brine salinity and composition, *Energy and Fuels* 17(5) (2003) 1133‑1144.

50. H. Roshan, M.S. Andersen, H. Rutlidge, C.E. Marjo, R.I. Acworth, Investigation of the kinetics of water uptake into partially saturated shales, *Water Resources Research* 52(4) (2016) 2420‑2438.

51. A.J.B. Milne, A. Amirfazli, The Cassie equation: How it is meant to be used, *Advances in Colloid and Interface Science* 170(1) (2012) 48‑55.